A hierarchical model of weak polyelectrolytes with ionization and conformation consistency

Alejandro Gallegos and Jianzhong Wu*

Department of Chemical and Environmental Engineering, University of California, Riverside, CA 92521, USA

Table of Contents Graphic

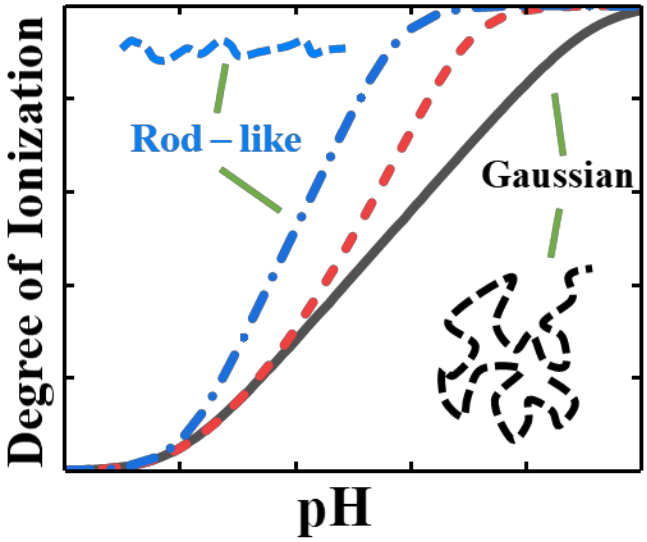

*To whom correspondence should be addressed. Email: jwu@engr.ucr.edu

Abstract

Conventional models of weak polyelectrolytes are formulated in terms of either an average degree of ionization or a rigid polymer conformation. While the decoupling of segment-level ionization and polymer structure simplifies the theoretical procedure and is beneficial from a computational perspective, it misses intra-chain correlations (i.e., interactions beyond adjacent monomers) that are important for systems at low polymer concentration with strong electrostatic interactions. In this work, we propose a hierarchical method that incorporates the liquid-state methods with the site-binding model to account for the effects of the local ionic environment on both inter- and intra-chain correlations. A worm-like chain model is introduced to describe the coupling of polymer conformation with monomeric ionization with the long-range electrostatic interactions accounted for by using the Gibbs-Bogoliubov variational principle. Through an extensive comparison of the theoretical predictions with experimental titration curves for poly(acrylic acid) in different alkali chloride solutions, we demonstrate that the hierarchical model is able to quantify the charging behavior of weak polyelectrolytes over a broad range of solution conditions.

Keywords:

Site-binding model, liquid-state theories, Gibbs-Bogoliubov variational principle

1. Introduction

Understanding the charging behavior of weak polyelectrolytes is critical to technological applications such as bioadhesion[1], drug delivery[2], wastewater treatment[3] and thermal energy storage[4]. In general, the performance of weak polyelectrolytes is dependent on the polymer charge and conformation as well as their responses to subtle variations in the local chemical environment. Due to the long-range nature of electrostatic interactions and intra-chain correlation effects and the

intrinsic coupling between polymer ionization and conformation changes, it remains a theoretical challenge to accurately describe weak polyelectrolytes in dilute solutions. Further theoretical development is needed for the rational design of "smart" polymeric systems to achieve their specific functionality such as targeted drug delivery and controlled release, taking advantage of the changes in the ionization and structure of the polymer backbone in response to variations in the pH and composition of the intracellular fluids.[2, 5]

Ionization of a weak polyelectrolyte in a liquid environment is dependent on the polymer conformation (and vice versa) because of intra-chain correlations. While the charge-conformation coupling is relatively insignificant at high polymer volume fractions or high salt concentrations due to the screening effects, the correlation effects are significant in dilute solutions as often encountered in practical applications. For weak polyelectrolytes at large salt concentrations, the site-binding model and its modifications have achieved great success to describe the titration of individual polymer chains by representing each polymer as a one-dimensional lattice of ionizable sites. Because the polymer segments are assumed to interact with each other only through the nearest neighbor segments,[6-8] the lattice model is not able to account for long-range electrostatic interactions and ignores the charge effects on polymer conformation. The long-range intra-chain interactions are particularly important at low electrolyte concentrations. In many cases, the good performance of the site-binding model is likely fortuitous owing to the use of adjustable parameters for different solution conditions.

We recently demonstrated that, coupled with a thermodynamic model for describing the solution non-ideality, a nearest-neighbor site-binding model (nnSB) can accurately represent weak polyelectrolyte titration at moderate to high salt concentrations using a single set of model parameter.[9] While the thermodynamic model allows for the prediction of site-binding parameters

in response to variations in the ionic strength, the theoretical performance deteriorates at low salt concentration because it ignores non-nearest-neighbor interactions among polymer segments. This failure highlights the importance of non-neighboring intra-chain interactions in regulating the charging behavior of dilute weak polyelectrolytes. While our model describes the thermodynamic non-ideality due to the intermolecular interactions reasonably well, the intramolecular interactions were truncated at the nearest-neighbor level similar to that in the conventional site-binding methods and, as such, the polymer conformation was immaterial to the ionization states of individual segments. The deficiency is expected because the coupling between the polymer conformation and long-range intra-chain interactions is most significant for weak polyelectrolytes in dilute salt solutions. The purpose of this work is to remedy this caveat such that the thermodynamic model can quantify both the conformation and ionization of weak polyelectrolytes across various salt concentrations.

Conventional site-binding models are not applicable to weak polyelectrolytes at a finite polymer concentration. For such systems, the theoretical calculations are mostly based on mean-field methods that account for the average charge density or, equivalently, the average degree of polymer ionization. The mean-field methods have received considerable attention in recent years leading to significant advancements in modeling weak polyelectrolytes in the bulk and under inhomogeneous conditions.[10-13] For example, the self-consistent field theory (SCFT) was used to investigate the ionization and conformation of linear and star-like weak polyelectrolytes.[14] The mean-field approach provides a reasonable prediction of the polymer conformation, but shows significant deviation from the experimental and simulation results for ionization in dilute electrolyte solutions. The poor performance is understandable because, like other mean-field methods, SCFT ignores long-range intramolecular correlations. Such effects are magnified for

weak polyelectrolyte systems at low salt concentrations due to strong Coulomb interactions. The mean-field methods become even more problematic at low polymer concentration because, in that case, both the polymer conformation and ionization behavior of weak polyelectrolytes are dominated by long-range intrachain correlations.

Recently, we developed Ising density functional theory (iDFT) that treats the polymer conformation and ionization on an equal standing through a multidimensional vector specifying both the polymer ionization state and spatial configuration.[15] While iDFT shows noticeable improvements over conventional mean-field methods for describing intrachain correlations, it is not currently applicable to dilute solutions of weak polyelectrolytes due to the theoretical and numerical difficulties in evaluating multibody correlations. To carry out iDFT calculations for weak polyelectrolytes, we also truncated the intrachain correlations at the nearest-neighbor level (the version of iDFT is referred to as iDFTnr). Because the excess Helmholtz energy is formulated by truncating the intramolecular correlations at the nearest-neighbor level, iDFTnr becomes inaccurate for polymer ionization at dilute electrolyte conditions when long-range intramolecular interactions are most relevant. In principle, Monte Carlo (MC) simulations are able to handle the coupling effects of the polymer ionization and conformation because the simulation accounts for both inter- and intra-molecular correlations exactly.[11, 16-17] For example, Laguecir and coworkers showed that MC results agreed well with the experimental data for the degree of ionization of poly(acrylic acid) using a freely-jointed hard-sphere chain model with the electrostatic interactions described through the screened Debye-Hückel (DH) potential.[18] Regrettably, the DH potential is problematic to account for the ion concentration effects at high salt concentrations and the computational burden to sample the ensemble space increases quickyly with the polymer chain

length. MC simulation is, in particular, computationally demanding when salt ions as well as the protons and hydroxyl ions are explicitly considered.

In this work, we propose a hierarchical model to describe the titration of weak polyelectrolytes by incorporating the liquid-state methods with a generalized site-binding model. Unlike typical mean-field methods, our theoretical model is able to account for both short- and long-range interactions within a single polymer chain explicitly. By considering the electric potential near the polymer surface, we are able to describe the free energy of ionization for individual segments in a local solution environment. As a result, the liquid-state methods allow us to capture the effects of solution conditions on the ionization of individual segments. Meanwhile, the generalized site-binding model accounts for both non-neighboring intra-chain correlations and conformation of the polymer that are ignored in the conventional mean-field methods.

In the remainder of this article, we will present the theoretical details and numerical results as follows. We first describe the generalized site-binding model that incorporates the polymer conformation and non-neighboring intrachain interactions. Next, we show how the solution conditions can be accounted for by using the liquid-state methods to describe the inter- and intra-molecular interactions and correlation effects governing the ionization and conformation of the polymer chain. Subsequently, we discuss how the long-range intrachain interactions can be described by a combination of the Gibbs-Bogoliubov variational principle and the worm-like-chain model. Together, these different methods are referred to as the hierarchical site-binding model (hSB) as we account for the polymer behavior from the segment (*viz*. interactions and ionization of individual segments) to the macromolecular level (viz., average charge and polymer conformation). After we have explained the methodology, the numerical results are discussed by

direct comparison with experimental titration curves for linear poly(acrylic acid) in different alkali chloride solutions. Lastly, we investigate further the ionization and the conformation of the weak polyelectrolytes at dilute and high salt conditions.

2. Thermodynamic model and methods

In this section, we first introduce a single-chain Hamiltonian for weak polyelectrolytes and discuss the relevance of each term in the Hamiltonian to the ionization and conformation of the polymer chain. The single-chain Hamiltonian can be understood as a generalization of the site-binding model to include the polymer flexibility and non-neighboring interactions. The liquid-state methods are then presented to account for the influence of solution conditions on the inter- and intra-chain interactions within the framework of an augmented primitive model of electrolyte solutions. Next, we use the Gibbs-Bogoliubov variational principle to decouple the Hamiltonian into a solvable nearest-neighbor model and a perturbation that accounts for the non-neighboring interactions. Lastly, a worm-like-chain model is adopted to describe how the polymer conformation affects the average distances between the ionizable sites by using an effective persistence length that depends on non-neighboring interactions and an entropic term due to the chain expansion.

2.1 *A generalized site-binding model*

The conventional site-binding model for describing the ionization of weak polyelectrolytes is built upon the one-dimensional Ising model.[19-20] With the assumption that the polymer chain takes a rod-like conformation, each ionizable site exists in one of two charge states (*viz*. charged or uncharged), reflecting the protonation of a basic group or deprotonation of an acidic group in a polymer chain.[21] The free energy of ionization depends on the solution pH, the intrinsic proton binding energy, and nearest-neighbor interactions. Later modifications of the site-binding model

account for intramolecular interactions beyond the nearest-neighbor segments but the chain conformation is typically assumed rigid (i.e., the distances between ionizable sites are exactly known).[22]

The conventional site-binding model can be generalized to include chain flexibility and non-nearest-neighbor interactions. Toward that end, consider a weak polyelectrolyte chain with *M* ionizable sites with a specific architecture (*e.g.*, linear or branched). The charge state of the polymer is fully specified by a multidimensional vector $\mathbf{S} = (s_1, s_2, ..., s_M)$, where $s_i = +1$ or 0 denotes the charge state for a basic site ($s_i = -1$ or 0 for an acidic site). In addition to the charge numbers (*viz*., valence $Z_i(s_i)$ of segment *i*), the chain conformation depends on the positions of all segments, $\mathbf{R} = (\mathbf{r}_1, \mathbf{r}_2, ..., \mathbf{r}_M)$. For a bulk solution of weak polyelectrolytes, the system is uniform thus we may locate one of the end segments (viz., segment 1) at the origin and specify the chain conformation by $\vec{R} \equiv \mathbf{R}(\mathbf{r}_1 = 0)$, which differentiates that from the inhomogeneous counterpart **R**. A unique feature of weak polyelectrolytes is that the polymer charge is a dynamic variable coupled with the conformation.

The titration of weak polyelectrolyte chains can be described by using the semi-grand canonical ensemble, i.e., the system of interest is in thermodynamic equilibrium with a reservoir at a fixed pH. For simplicity, we consider a single weak polyelectrolyte chain consisting of only one type of ionizable groups (e.g., either polyacid or polybase). The procedure can be easily extended to bulk systems with a finite weak polyelectrolyte concentration. For each polymer conformation, we can evaluate the degree of ionization from the semi-grand canonical partition function similar to that in the conventional site-binding model

$$\Xi\left(\vec{R}\right)=\sum_{\mathbf{S}'}\exp\left[-\beta\Gamma\left(\vec{R},\mathbf{S}'\right)\right] \tag{1}$$

where $\beta^{-1}=k_BT$, k_{B} and T are the Boltzmann constant and absolute temperature, respectively. In our generalized site-binding model, the polymer is treated as flexible. Therefore, the grand potential is determined by integration over all possible polymer conformations, $\Omega=-\ln\int\Xi(\vec{R})d\vec{R}$

.

We assume that a weak polyelectrolyte can be represented by a tangentially connected chain with M hard spheres of equal diameter. The single-chain Hamiltonian can be written as

$$\Gamma\left(\vec{R},\mathbf{S}\right)=V^B\left(\vec{R}\right)+\sum_{i=1}^{M}\lambda_i\mid s_i\mid+\sum_{i=1}^{M-1}W_{i,i+1}\mid s_i\mid\mid s_{i+1}\mid+\sum_{i=1}^{M-2}\sum_{j>i+1}^{M}\Psi_{i,j}\left(r_{i,j}\right)\mid s_i\mid\mid s_j\mid. \tag{2}$$

For convenience, we have taken the absolute value of the segment state(s) so that the acidic or basic monomers can be treated on an equal footing. The first term on the right side of Eq.(2), $V^B(\vec{R})$, represents the bond potential

$$\exp\left[-\beta V^B\left(\vec{R}\right)\right]=\left[\prod_{i=1}^{M-1}\frac{\delta\left(\mid\mathbf{r}_{i+1}-\mathbf{r}_i\mid-\sigma\right)}{4\pi\sigma^2}\right]\exp\left[\beta\xi\sum_{i=1}^{M-1}\frac{\left(\mathbf{r}_{i+2}-\mathbf{r}_{i+1}\right)\cdot\left(\mathbf{r}_{i+1}-\mathbf{r}_i\right)}{\sigma^2}\right]. \tag{3}$$

Similar to the freely-rotating chain (FRC) model, the one-dimensional Dirac-delta function ensures a fixed bond length between the neighboring segments (viz., a tangent chain), and the exponential term accounts for an energy penalty when two consecutive bonds are not in parallel (i.e., the bending energy). In this work, we assume that there is no intrinsic stiffness to the polymer chain when the polymer is fully uncharged (viz., $\xi=0$), i.e., the polymer behaves as a freely jointed chain in the neutral state. As the polymer segments become ionized, the intrachain repulsion may

be represented by an effective stiffening parameter ξ^{eff}. In Section 2.4, we will discuss the chain conformation in more details.

The first summation on the right side of Eq.(2) accounts for the free energy change due to proton binding (or release from the polymer) as well as the difference in the excess chemical potential between charged and neutral segments. The one-body term is attributed to ionization equilibrium and the interaction of the polymer segment with other chemical species in the solution. The second and third terms on the right side of Eq.(2) account for the fact that the monomer interacts with both nearest and non-nearest neighbors due to the chain connectivity. The intramolecular interactions depend on the ionization states of segments *i* and *j* as well as the distance between them ($r_{i,j} = |\mathbf{r}_j - \mathbf{r}_i|$). Parameters λ_i, $W_{i,i+1}$, and $\Psi_{i,j}$ depend on the solution condition. We will show in the following subsection how these parameters are derived from a thermodynamic model for weak polyelectrolytes.

2.2 ***Solution effects***

To capture the polymer behavior at different solution conditions, we must quantify segment-segment interactions that define the parameters of the generalized site-binding model (viz., λ_i, $W_{i,i+1}$, $\Psi_{i,j}$, etc.). In this subsection, we introduce a molecular thermodynamic model to account for the effect of thermodynamic non-ideality on the titration behavior of weak polyelectrolytes.

Similar to our previous work for various ionizable systems[9, 15, 23-24], we employ an augmented primitive model (APM) for polyelectrolyte solutions to account for electrostatic interactions and various forms of short-range interactions. The polymer segments are represented by hard spheres that can be either charged or neutral depending on ionization state. We assume

that the separation between the nearest-neighboring segments is the same as the hard-sphere diameter (viz., a tangent chain). For simplicity, the hard-sphere diameter of polymer segments is assumed not dependent on the ionization state or salt concentration. Unlike alternative coarse-grained models of polyelectrolytes, the salt ions, protons, and hydroxyl ions are explicitly considered as charged hard spheres. The hydrated diameters for the salt ions were taken from Simonin et al.[25] (*viz.* $\sigma_{Li^+} = 4.76\,\text{Å}$, $\sigma_{Na^+} = 3.90\,\text{Å}$, $\sigma_{K^+} = 3.34\,\text{Å}$, $\sigma_{Cs^+} = 1.89\,\text{Å}$, and $\sigma_{Cl^-} = 3.62$ Å) and Gallegos et al.[24] (*viz.* $\sigma_{H^+} = 5.00\,\text{Å}$ and $\sigma_{OH^-} = 3.22\,\text{Å}$). The polymer and salt ions are immersed in a continuum medium with a dielectric constant representative of liquid water at room temperature ($\varepsilon_r = 78.4$). Charge neutrality of the solution is maintained by addition of salt cations or anions to compensate for the difference in the proton and hydroxyl ions.

Thermodynamic non-ideality plays an important role in both the one- and two-body potentials employed in our generalized site-binding model. In the conventional nearest-neighbor model, λ_i and $W_{i,i+1}$ are treated as adjustable parameters changing with the solution condition. In this subsection, we show that these terms can be predicted from APM.

2.2.1 One-body potential

The one-body potential arises exclusively from the interaction of a polymer segment and the background solution. It depends on the difference in intermolecular interactions between the charged and uncharged state of the monomer as well as a contribution due to the binding energy of the proton:

$$\lambda_i = -s_i k_B T \left(\mathrm{pK}_i - \mathrm{pH}\right) \ln 10 + \Delta\mu_i^{mon} + \Delta\mu_i^{ch} \tag{4}$$

where the first term on the right is affiliated with the change in free energy due to the binding of a proton, the middle term results from change in intermolecular interactions of segment *i* with all other monomers and ions in the system due to its ionization, and the last term arises from the change in the excess chemical potential of segment *i* due to chain connectivity. At a finite polymer concentration, the latter describes the change in intrachain correlation energy for all chains due to segment *i* when it is ionized. Within APM, the monomeric contribution μ_i^{mon} can be decomposed into an excluded volume term $\Delta\mu_i^{hs}$, a contribution due to electrostatic correlations $\Delta\mu_i^{el}$, and additional contributions if other solvent-mediated interactions are included. In this work, $\Delta\mu^{ch}$ can be omitted because we consider weak polyelectrolyte titration in the single-chain limit ($\Delta\mu^{ch}$ is proportional to the polymer density and thus vanishes in the dilute limit).

The negative logarithm of the equilibrium constant for the ionization reaction [i.e., pK_i in Eq.(4)] depends on the identity of the ionizable site and temperature, but not on the solution composition. As mentioned above, $s_i = +1$ corresponds to the protonation of a weak basic segment, and $s_i = -1$ for the deprotonation of a weak acidic segment. For all calculations in this work, we adopt the pK_i value for the acrylic acid monomer (viz., $pK_i = 4.756$[26]). The hard-sphere component $\Delta\mu_i^{hs}$ is only relevant when the hard-sphere diameter of the monomer varies with the ionization state (e.g., due to the change in hydration). Typically, this term is important only in highly concentrated electrolyte solutions and therefore, for simplicity, we assume the hard-sphere diameter is independent of the ionization state (i.e., $\Delta\mu_i^{hs} = 0$).[24]

The electrostatic correlations term, $\Delta\mu_i^{el}$, arises from the non-uniform distribution of free ions and other polymer segments around a charged monomer. This term can be calculated by

using the mean-spherical approximation (MSA).[27] MSA captures the finite-size effect of ions on the electrostatic interactions while reducing to the Debye-Hückel (DH) limiting law at dilute electrolyte concentrations.[28] According to MSA, the change in the excess chemical potential of segment *i* due to ionization is given by

$$\beta\Delta\mu_i^{el} = -l_B\left[\frac{\Gamma^{MSA}}{1+\Gamma^{MSA}\sigma_i} + \frac{2Z_i\eta\sigma_i}{1+\Gamma^{MSA}\sigma_i}\right] \tag{5}$$

where $l_B = \beta e^2 / 4\pi\varepsilon_0\varepsilon_r$ is the Bjerrum length (7.14 Å for liquid water at room temperature), *e* is the elementary charge; ε_0 and ε_r are the vacuum permittivity and dielectric constant of the solvent, respectively; σ_i and Z_i are the hard-sphere diameter and valence of the charged monomer; η is a parameter related to the ionic asymmetry (i.e., differences in size and valence of the ionic species); and Γ^{MSA} is the MSA screening parameter. Approximately, Γ^{MSA} is proportional to the square root of the ionic strength similar to that for the Debye screening parameter. As a result of this square root dependency, the importance of electrostatics becomes relevant even at dilute conditions (which will be seen in the two-body terms as well).

2.2.2 Intrachain potential

In addition to the one-body potential, the solution condition affects the nearest-neighbor energy, $W_{i,i+1}$, and non-neighboring energy, $\Psi_{i,j}$, used in the generalized site-binding model. The intrachain potential accounts for the free-energy cost to ionize segment *i* given that segment *j* in the same polymer chain is already ionized. It is different from the intermolecular interactions discussed above that are accounted for by the one-body potential λ_i.

As shown in our previous work,[9] the nearest-neighbor interaction can be decomposed into two contributions: $W_{i,i+1} = -\ln g^{el}_{i,i+1}(\sigma) + u_{i,i+1}(\sigma)$ where the first term accounts for the electrostatic work to bring to charged segments from infinity to contact (i.e., to form an ionic bond), and the second term is non-electrostatic in origin and accounts for specific interactions (e.g., breakdown of intramolecular hydrogen bonding[29]). While a quantitative prediction of the non-electrostatic energy is difficult to achieve from a molecular perspective, we expect that the short-range interaction is relatively insensitive to solution conditions. In this work, the non-electrostatic component $u_{i,i+1}$ is estimated by fitting the experimental data across different solution conditions and the value determined is used as the non-electrostatic energy between all paired segments. A generalization of the nearest-neighbor interaction expression to account for non-neighboring interactions results in $\Psi_{i,j}(r_{i,j}) = -\ln g^{el}_{i,j}(r_{i,j})$ where we have neglected the non-electrostatic component since these are typically short-ranged. Thus, the electrostatic component of the two-body interactions ($W_{i,i+1}$ and $\Psi_{i,j}$) are treated at the same level through the radial distribution function which accounts for the electrostatic work to place two charges separated at a distance $r_{i,j}$ in the solution.

The usual choice for the electrostatic interaction between charges in a solution follows from the Debye-Hückel potential

$$\beta \Psi_{i,j}\left(r_{i,j}\right) = \frac{l_B}{r_{i,j}} Z_i Z_j \exp\left[-\kappa r_{i,j}\right]. \tag{6}$$

While Eq.(6) is convenient in theoretical development, the DH potential is valid only for dilute electrolyte systems.[18] While the DH potential captures qualitatively the long-range nature of Coulomb interactions and the screening effect resulting from salt ions through the DH parameter

κ, it is unable to capture salt-specific effects responsible for the differences in the titration behavior of weak polymers in different electrolyte solutions.[30] Intuitively, one can expect that there is an accumulation of counterions within the vicinity of the charged polymer that leads to a stronger electrostatic screening than that expected from the bulk salt concentration. The local ion concentration near the polymer depends on the degree of ionization and electrostatic interactions between the polymer segments and the surrounding ions. The local electric potential is not easily determined without expensive computational procedures such as iDFT.[15]

To account for long-range intra-chain interactions, we first determine the local electric potential of a weak polyelectrolyte (WPE) using a test particle method

$$\phi_{WPE}^{local} \approx \phi_{mon}^{local} \times \alpha_{WPE}, \tag{7}$$

where ϕ_{mon}^{local} is the electrostatic potential at the surface of an isolated charged monomer (i.e., test particle) in the background salt solution, and α_{WPE} is the average degree of ionization for the polymer. In principle, the local electric potential is segment-dependent (i.e., the electric potential is not constant along the polymer chain); however, such considerations would be cumbersome from a computational perspective. Alternatively, we may determine the electrostatic potential at the surface of the isolated charged monomer by fixing a particle of absolute charge *e* and hard-sphere diameter σ_i at the origin.[31] Additional details on the electrostatic potential for the monomer can be found in the SI.

With an approximate local electric potential for the entire polymer, we can estimate the local concentration for each ion from the Boltzmann equation

$$c_i^{local} = c_i \exp(-\beta e Z_i \phi_{WPE}^{local}) \tag{8}$$

where c_i and Z_i are the bulk concentration and valence of ion *i*. A general trend to note is that when the polymer is uncharged, the local counterion concentration is similar to that in the bulk. As the polymer charge increases, the counterions will accumulate at the surface at a rate dependent upon the electrostatic driving force (i.e., ϕ_{mon}^{local}). The strength of the driving force is greatest at dilute salt concentrations when the electrostatic screening is weakest. Thus, at high salt concentration, the electrostatic potential for the monomer will be small and the local concentration of ions will be only slightly greater than the bulk solution. As a result of this modification, the DH parameter κ is replaced by the local DH parameter $\kappa^{local} = \sqrt{4\pi l_B \sum_i c_i^{local} Z_i^2}$.

In addition to ion concentration in the vicinity of the ionizable polymer, we must account for the salt-dependence of the long-range interactions. Experimental titration data for poly(acrylic acid) indicates that the ionization behavior of the polymer at low salt concentration is sensitive to the choice of counterions.[30] In order to capture the ion-specific effect, we introduce an empirical parameter τ_{cat^+} that modifies the strength of electrostatic screening. The long-range intrachain repulsion is strengthened in the presence of more hydrated ions (viz. lithium and sodium) than its less hydrated counterparts (viz. potassium and cesium). It seems that the intrachain repulsion is partially enhanced by the excluded volume of counterions with a large hydration shell.

Within the framework of the charged hard-sphere model, we can approximate the two-body electrostatic potential between ionizable segments in the same polymer chain by[32]

$$-\ln g_{i,j}^{el}\left(r_{i,j}\right) = \frac{l_B}{r_{i,j}} \frac{Z_i - \eta\sigma^2}{1+\Gamma^{MSA}\sigma} \frac{Z_j - \eta\sigma^2}{1+\Gamma^{MSA}\sigma} \exp\left[-\tau_{cat^+}\kappa^{local}\left(r_{i,j}-\sigma\right)\right] \tag{9}$$

where c_s^{local} is the local salt concentration, and τ_{cat^+} is the aforementioned screening parameter. It should be noted that at the nearest-neighbor level (i.e., $r_{i,j} = \sigma$), the electrostatic contribution is

equivalent to the expression used in our previous work since the exponential factor will be exactly unity.[9] At infinite dilution, the radial distribution function reduces to the exponential of the negative value of the electrostatic pair potential (*i.e.*, $-\ln g_{i,j}^{el}(r_{i,j}) = l_B Z_i Z_j / r_{i,j}$). Using Eq.(9) to calculate the two-body electrostatic potential, we are able to account for the intrachain interactions between charged monomers at dilute salt conditions. Note that Eq.(9) does not reduce to the DH limit for large *r* due to the presence of τ_{cat^+} in the exponential term and the use of the local salt concentration in κ^{local}. As discussed above, the DH potential is not valid for strongly correlated systems and does not account for ion-specific effects. Although the modification of the potential of mean force from MSA with τ_{cat^+} is strictly empirical, Eq.(9) allows us to capture non-neighboring intrachain interactions and specific effects of salt ions.

As discussed above, while the nearest-neighbor term has shown to be sufficient at capturing the titration behavior of polyacids in moderate to high salt concentrations, it misses the long-range interactions among segments from the same polymer chain. As a result, the titration behavior is noticeably overpredicted in dilute solutions because the additional resistance to ionization due to the long-range interactions is not accounted for in the nearest-neighbor Hamiltonian. Thus, the inclusion of non-neighboring interactions between segments is a necessary feature to our model because we can capture the weak polyelectrolytes even at dilute conditions where the nearest-neighbor model fails. In the following subsections, we will demonstrate a method to include these long-range interactions and the coupling with the polymer conformation.

2.3 *Incorporating long-range interactions*

In this subsection, we introduce a coarse-grained procedure for describing non-neighboring intrachain interactions in weak polyelectrolyte systems following the so-called local effective

interaction parameters (LEIP) method developed by Blanco and coworkers.[22, 33-35] For the generalized site-binding model, we split the single-chain Hamiltonian in Eq.(1) such that the potential for the interaction between the non-neighboring segments is separated from the other terms

$$\Gamma(\vec{R},\mathbf{S}) = \hat{\Gamma}_0(\vec{R},\mathbf{S};\{x_i\}) + \Delta\hat{\Gamma}(\vec{R},\mathbf{S};\{x_i\}) \tag{10}$$

where the reference Hamiltonian is composed of a bond potential and the nearest-neighbor energy

$$\hat{\Gamma}_0\left(\vec{R},\mathbf{S};\{x_i\}\right) = V^B\left(\vec{R}\right) + \Gamma_{nn}\left(\mathbf{S};\{x_i\}\right) \tag{11}$$

with

$$\Gamma_{nn}\left(\mathbf{S};\{x_i\}\right) = \sum_{i=1}^{M}\left(\lambda_i + x_i\right)|s_i| + \sum_{i=1}^{M-1} W_{i,i+1}|s_i||s_{i+1}|. \tag{12}$$

The non-neighbor potential is given by

$$\Delta\hat{\Gamma}\left(\vec{R},\mathbf{S};\{x_i\}\right) = \sum_{i=1}^{M-2}\sum_{j>i+1}^{M}\Psi_{i,j}\left(r_{i,j}\right)|s_i s_j| - \sum_{i=1}^{M} x_i|s_i| \tag{13}$$

where $\{x_i\}$ represent a set of one-body potentials yet to be determined. Importantly, the reference Hamiltonian $\hat{\Gamma}_0$ depends on the polymer conformation only through the bond potential. It varies with the ionization state of individual segments through the one-body potential $(\lambda_i + x_i)$ and nearest-neighbor energy ($W_{i,i+1}$).

The Gibbs-Bogoliubov inequality [36] states that the true grand potential Ω, i.e., one that takes into account explicitly the coupling of ionization and conformation, has an upper bound $\Omega \le \hat{\Omega}$ where

$$\hat{\Omega} \equiv \hat{\Omega}_0\left(\{x_i\}\right) + \left\langle \Delta\hat{\Gamma}\left(\vec{R}, \mathbf{S}; \{x_i\}\right)\right\rangle_0 \tag{14}$$

where $\langle\cdots\rangle_0$ represents the ensemble average with respect to the reference Hamiltonian $\hat{\Gamma}_0$. Importantly, the Gibbs-Bogoliubov inequality has decoupled the non-neighboring interactions (which are problematic to incorporate) from the reference system in which the conformation and ionization of the polymer are independent from one another. The grand potential for this reference system is given by

$$\hat{\Omega}_0\left(\{x_i\}\right) = -k_B T \ln \int \sum_{\mathbf{S}} \exp[-\beta \hat{\Gamma}_0(\vec{R})]\, d\vec{R} \tag{15}$$

For convenience, here we introduce the nearest-neighbor partition function $\hat{\Xi}_0(\{x_i\}) = \sum_{\mathbf{S}} \exp\left[-\beta \Gamma_{nn}(\mathbf{S}; \{x_i\})\right]$ as used in the conventional site-binding model. This allows us to write the reference grand potential as the sum of the ionization and conformation components

$$\hat{\Omega}_0(\{x_i\}) = -k_B T \ln \hat{\Xi}_0(\{x_i\}) - k_B T \ln \int \exp[-\beta V^B(\vec{R})] d\vec{R}\,. \tag{16}$$

The second term on the right side of Eq.(16) corresponds to the partition function of an ideal chain, which can be evaluated analytically

$$\hat{\Omega}_0(\{x_i\}) = -k_B T \ln \hat{\Xi}_0(\{x_i\}) + \int d\vec{R} p(\vec{R}) \left[k_B T \ln p(\vec{R}) + V^B(\vec{R})\right] \tag{17}$$

where $p(\vec{R}) = \exp[-\beta V^B(\vec{R})] / \int \exp[-\beta V^B(\vec{R})] d\vec{R}$ is defined in terms of the conformation of a neutral chain with only the bond energy. Eq.(17) indicates that the grand potential of the reference system depends on the nearest-neighbor interactions as well as the polymer conformation. As discussed in the following, we can evaluate the statistics of polymer conformations by mapping the weak polyelectrolyte into a worm-like chain.

To relate the long-range intrachain interactions with the conformation, we follow Flory's uniform expansion model.[37] With the assumption that the intrachain interactions result in a uniform expansion of the polymer backbone (i.e., all parts of the chain are considered to have their mean dimensions changed by exactly the same factor), we can estimate the probability distribution function for the end-to-end vector r_{ee} (or $r_{1,M}$ in our tangent chain model) $p_\upsilon\left(r_{ee}\right)$ from that of an unperturbed Gaussian chain $p(r_{ee})$, i.e., $p_\upsilon(r_{ee}) = \upsilon^3 p(\upsilon r_{ee})$, where the expansion factor υ is defined as the thermally averaged end-to-end distance of the uniformly expanded polymer normalized by the thermally averaged end-to-end distance of an ideal chain, $\upsilon^2 = \langle r_{1,M}^2 \rangle_0 \big/ (M-1)\sigma^2$. The factor υ^3 is required for normalization of the conformation probability. Accordingly, the change in the free energy a single polymer system can be determined based on the ideal chain expression after further averaging over $\vec{R}$ (in the unperturbed Gaussian chain state)[38-40]

$$F^{ent}\left(\vec{R}_0\right) = -k_B T\left[\frac{3}{2}(M-1)\ln\left(1-\frac{\upsilon^2}{M-1}\right)-3\ln\upsilon\right]. \tag{18}$$

Here, $\vec{R}_0$ represents the polymer configuration after the thermal average. In the uniform expansion model, it is described in terms of the end-to-end distance $\langle r_{1,M}^2 \rangle_0$. The first term on the right-hand side of Eq.(18) represents the entropic contribution due to the compression of the polymer chain while the second term arises from the resistance to chain compression as deduced by Flory.[41-42] A combination of contributions from the ionization and chain conformation leads to the reference grand potential

$$\widehat{\Omega}_0(\vec{R}_0, \{x_i\}) = -k_B T \ln \widehat{\Xi}_0(\{x_i\}) + F^{ent}\left(\vec{R}_0\right). \tag{19}$$

The first term on the right side of Eq.(19) represents the free energy due to the ionization and nearest-neighbor interactions, and the second term accounts for the conformation of ideal chains. Eq.(19) allows us to determine the grand potential of the reference system based on parameters x_i and υ (or similarly $\vec{R}_0$) without sampling the polymer conformations explicitly. The determination of these parameters depends on the non-neighboring potential $\Delta\widehat{\Gamma}$ yet to be discussed.

Because the one-body and nearest-neighbor potentials are decoupled from the polymer conformations, we can evaluate the ensemble average of $\Delta\widehat{\Gamma}$ based on the reference system analytically (see SI)

$$\left\langle \Delta\Gamma\left(\vec{R},\mathbf{S};\{x_i\}\right)\right\rangle_0 = \sum_{i=1}^{M-2}\sum_{j=i+2}^{M}\Psi_{i,j}\left(\hat{r}_{i,j}\right)\hat{h}_{i,j} - \sum_{i=1}^{M} x_i\hat{\alpha}_i \tag{20}$$

where $\hat{\alpha}_i = \langle |\, s_i \,| \rangle_0$ and $\hat{h}_{i,j} = \langle |\, s_i \,||\, s_j \,| \rangle$ are the degree of ionization for segment *i* and the correlation function for segments *i* and *j* in the reference system, respectively. Note that the ensemble average of the non-neighboring component shown in Eq.(20) is an approximate of the true ensemble average when non-neighboring interactions were considered explicitly. If the nearest-neighbor interactions were not considered explicitly, the site-site correlation function would be given by $\hat{h}_{i,j} = \langle |\, s_i \,||\, s_j \,| \rangle_0 = \langle |\, s_i \,| \rangle_0 \langle |\, s_j \,| \rangle_0 = \hat{\alpha}_i\hat{\alpha}_j$. Note that the non-neighboring interaction depends on the distance between sites $\hat{r}_{i,j}$ after thermal average. The coupling between polymer conformation and ionization represents a key feature of our heirarchical model. We will discuss the determination of $\hat{r}_{i,j}$ in the following subsection.

With the analytical expressions for refernce and perturbation free energies discussed above, we can determine parameters $\{x_i\}$ through a minimization scheme. Specifically, we choose x_i such that it minimizes the upper bound of the grand potential given by Eq.(14), $\partial\widehat{\Omega}/\partial x_i = 0$. Because x_i is affiliated with the change in free energy due to non-neighboring intrachain interactions resulting from the ionization of segment *i*, the variational principle implies (given that optimal values for $\{x_i\}$ are used) that all thermal averages (e.g., degree of ionization, correlation functions, etc.) can be evaluated by replacing the thermal average $\langle\cdots\rangle$ by $\langle\cdots\rangle_0$. In this work, we determine these mean-field parameters numerically through a high-dimensional optimization scheme. For the longest chain considered in this work (viz., *M*=1200), we evaluate the nearest-neighbor site-binding model by assuming that all monomers are equivalent (i.e., we ignore end-effects)[22]. At large chain lengths, the end-effects have less effects on the overall properties of the polymer. As a result, there is no need to perform optimization with respect to all $\{x_i\}$ because the segments are assumed equivalent. The assumption of $x_i = \overline{x}_i$ greatly simplifies the numerical determination of the one-body mean-field parameter. We show how to determine the degree of ionization and site-site correlation function with this simplification in SI. Note that although all monomers are treated equivalently, correlation still exists between charged sites (i.e., $\widehat{h}_{i,j} \neq \widehat{\alpha}_i\widehat{\alpha}_j$) because the intrachain interactions are considered only without end effects. Alternatively, we may implement the Gibbs-Bogoliubov variational principle without an explicit evaluation of the mean-field parameters (see SI for details).

The Gibbs-Bogoliubov variational principle allows us to incorporate the non-neighboring interactions by using the nearest-neighbor model as a reference. While a similar method was employed previously by Blanco and coworkers,[22, 33-35] the original work did not account for the

effects of solution conditions on the one-body and two-body terms, λ_i and $W_{i,i+1}$. In addition, the polymer conformation was evaluated through the rotational isomeric state (RIS) model[33] or by simulating the stretching of the chain[34]. In this work, we describe the solution conditions and the inter- and intra-molecular interactions through a molecular thermodynamic model (Section 2.2). We also account for the polymer conformation through $\hat{r}_{i,j}$, which is determined by a worm-like chain model to be discussed in the next subsection.

2.4 ***Spatial configuration of weak polyelectrolytes***

To establish a connection between intrachain interactions and the polymer conformation, we adopt a worm-like chain (WLC) model to approximate the conformation of a freely jointed chain with long-range intrachain interactions. In other words, the WLC model is used to represent the polymer expansion due to both excluded volume effects and long-range electrostatic interactions. Assuming that the segment diameter is the same as the segment-segment distance in the WLC, the distance between non-neighboring ionizable groups *i* and *j* can be expressed in terms of the segment diameter and effective persistence length

$$\hat{r}_{i,j}^2 = \left\langle r_{i,j}^2 \right\rangle_0 = 2\ell^{eff}\left(j-i\right)\sigma\left\{1-\frac{\ell^{eff}}{\left(j-i\right)\sigma}\left[1-\exp\left(-\frac{\left(j-i\right)\sigma}{\ell^{eff}}\right)\right]\right\}. \tag{21}$$

Since the non-neighboring interactions depend on the thermal average distance between monomers, $\langle r_{i,j}^2\rangle_0$, which is a function of the effective persistence length ℓ^{eff}, there is a coupling between the ionization state of the polymer and the polymer expansion. Note that ℓ^{eff} is related to the mean polymer configuration, $\vec{R}_0$, and the expansion factor υ through minimization of the grand potential. In other words, we determine the effective persistence length ℓ^{eff} by minimization

of the upper bound of the true grand potential $\widehat{\Omega}$, i.e., $\partial\beta\widehat{\Omega}/\partial\ell^{eff}=0$. The conformation entropy of the polymer chain [see Eq.(18)] is determined by substituting the end-to-end distance determined from Eq.(21). Besides the end-to-end distance, the WLC model also allows us to determine the radius of gyration

$$\left(R_g^{WLC}\right)^2=\frac{(M-1)\ell^{eff}\sigma}{3}-\left(\ell^{eff}\right)^2\left\{1-\frac{2\ell^{eff}}{(M-1)\sigma}+2\left[\frac{\ell^{eff}}{(M-1)\sigma}\right]^2\left[1-\exp\left(\frac{(M-1)\sigma}{\ell^{eff}}\right)\right]\right\}. \quad (22)$$

Eq.(22) gives the correct limiting behavior for the radius of gyration of an ideal Gaussian chain and rod-like chain (viz. $R_g^{ideal}=\sigma\sqrt{(M-1)/6}$ and $R_g^{rod}=\sigma(M-1)/\sqrt{12}$, respectively).

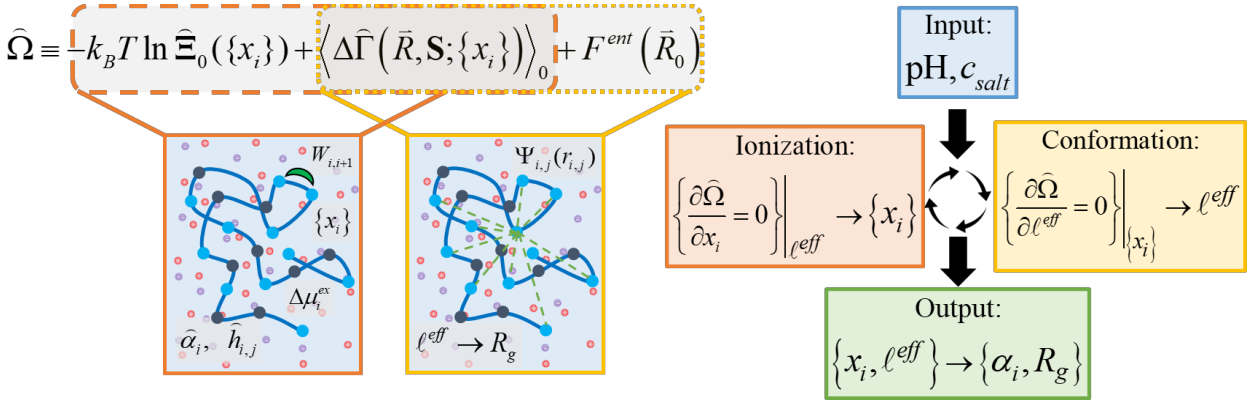

Figure 1. A schematic of the hierarchical model for the charge regulation of a weak polyelectrolyte chain. The ionization-conformation consistency is achieved through the integration of the site-binding model with a worm-like chain model to describe site-site distance and the liquid-state theory to account for solution conditions.

To summarize our theoretical procedure, we present in Figure 1 a schematic flow chart to determine the ionization and conformation behavior of a weak polyelectrolyte chain. The hierarchical model employs a generalized site-binding model to describe the Hamiltonian of weak polyelectrolytes in their different ionization states. Unlike the conventional nearest-neighbor site-

binding model, we consider additional contributions to the Hamiltonian due to the non-neighboring interactions between ionizable sites and polymer flexibility. While usually the inclusion of non-neighboring interactions is computationally expensive, we take advantage of the Gibbs-Bogoliubov inequality to approximate the non-neighboring interactions (i.e., the interaction of a segment with all other segments is described by a perturbation expansion). In addition, the conformation of the polymer is coupled to the ionization of the polymer by employing a worm-like chain model. By minimizing the free energy in terms of an effective persistence length ℓ^{eff}, we are able to calculate the separation between ionizable segments self-consistently. Importantly, the hierarchical model accounts for the effects of solution conditions on the one-body term, λ_i, and the two-body terms, $W_{i,i+1}$ and $\Psi_{i,j}$, through a molecular thermodynamic model of electrolyte solutions. The combination of segment-level correlation effects and intra-chain correlations allows us to determine the ionization and conformation behavior of weak polyelectrolytes at arbitrary solution conditions.

3. Results and Discussion

In the following, we illustrate the intra-chain correlation effects on the conformation and the ionization behavior of weak polyelectrolytes. For the calibration of theoretical results, our discussion is focused on the aqueous solutions of poly(acrylic acid) in presence of different counterions. PAA is a linear polymer with a relatively low density of ionizable groups. At medium to high salt concentrations, the weak interaction between monomers leads to a titration curve that exhibits a smooth transition from the fully uncharged state to the fully charged state. Unlike that for strongly correlated weak polymers such as poly(maleic acid)[29], PAA ionization lacks a step-like feature in the titration curve. Its titration behavior has been well studied using different experimental[30, 43-45] and computational methods[46-48]. The experimental results can be reasonably

described with various mean-field approximations owing to the weak interactions between neighboring sites[21, 30, 49]. However, as discussed above and demonstrated in our previous work[9], the truncation of intramolecular correlations to the nearest-neighbor (or completely neglecting the correlation effects like in some mean-field theories) results in a poor description of ionization at low salt conditions[15]. In this work, we demonstrate a more comprehensive model that fully captures the ionization and conformation behavior of the weak polyelectrolyte at all solution conditions.

Our thermodynamic model employs two parameters, τ_{cat^+} and $u_{i,i+1}$, that are obtained by matching the experimental data. As discussed above, the effective screening parameter and the non-electrostatic energy account for specific ionic effects and are dependent on the salt counterion, not salt concentration. Table 1 presents the numerical values for all parameters used to capture the experimental data. In addition to salt-dependent parameters, the terms, pK_i and σ_i, are the thermodynamic equilibrium constant and the hard-sphere diameter of each segment, respectively. These parameter are intrinsic to the polymer and are assumed the same for all monomers in the poly(acrylic acid) chain (i.e., no difference in the monomer position or chain length). Unlike the parameters employed in the conventional nearest-neighbor model, all parameters in our model are independent of the solution conditions (viz. pH and salt concentration). In particular, the thermodynamic equilibrium constant and monomer size are the same for all alkali metals (i.e., independent of the specific salt present in the solution).

Table 1. Model parameters for describing the ionization and conformation of poly(acrylic acid) in different salt solutions.

Poly(acrylic acid)	Intrinsic parameters	Salt-dependent parameters	τ_{cat^+}	$u_{i,i+1}$ (k_BT)

pK_i	4.756	LiCl	0.257	-0.053
σ	4.874 Å	NaCl	0.273	0.081
		KCl	0.462	0.507
		CsCl	0.857	0.594

To minimize the number of unknown variables, the pK_i value for PAA is assumed the same as that of the free monomer acrylic acid (viz. $pK_i = 4.756$[26]). Therefore, our model is equally applicable to ionization in the single monomer limit. This contrasts with our previous work using a nearest-neighbor model where the pK_i value was used as an adjustable parameter and determined to be significantly larger the monomeric value (viz. $pK_i = 5.22$)[9]. The larger value is not surprising since the long-range interactions were not included in the nearest-neighbor model and such interactions inhibit polymer ionization. The hard-sphere diameter of monomers is an important parameter in our model because it governs the distance between neighboring sites. In the nearest-neighbor model, it was necessary to fit σ_i for PAA at different salt solutions (e.g., LiCl vs CsCl) in order to capture the experimental titration curves. In this work, we determine the hard-sphere diameter based off the excluded volume calculated by the molecular model of PAA using the Molinspiration Cheminformatics 2018 software package (http://www.molinspiration.com). The estimated volume for a monomer in PAA was 60.63 $Å^3$ which corresponds to a hard-sphere diameter of $\sigma_i = 4.874$ Å. Thus, our model is free of fitting parameters for the intrinsic properties of the polymer (i.e., pK_i and size).

We find that the non-electrostatic energy and the effective screening parameter to be dependent on the specific salt cation present in the solution. Since our coarse-grained model does not account for specific chemical effects due to solvation, we expect that these parameters reflect such effects in an approximate manner. Because cation hydration is highly dependent upon the

Pauling radius ($\sigma_{hyd} \sim 2/\sigma_{Pauling}$)[50], the adsorption of cations to PAA is expected to have major impacts on the local water structure and the segment-segment interactions. The local modulation of the water structure could contribute to the repulsive non-electrostatic energy between neighboring sites. We find that the presence of strongly hydrated cations leads to less non-electrostatic intrachain repulsion between neighboring monomers than the cations that are less hydrated. In fact, the most hydrated counterion, Li^+, shows a very weak non-electrostatic attraction between two charged sites (note that this contribution is much less than the electrostatic repulsion). The adsorption of the ions with small hydration shells near the neighboring charged sites may interrupt local intermolecular hydrogen bonding between the displaced water molecules and the functional groups. The non-electrostatic energy $u_{i,i+1}$ was determined to be -0.064, 0.081, 0.507, and 0.594 k_BT for PAA in aqueous solutions of LiCl, NaCl, KCl, and CsCl, respectively. There is a significant difference in $u_{i,i+1}$ between Na^+ and K^+ while the values are similar for K^+ and Cs^+. These trends follow from more hydrated nature of Li^+ and Na^+ whereas K^+ and Cs^+ are minimally hydrated. When cations are adsorbed near the polymer surface, Li^+ and Na^+ ions have little influence on the hydrogen bonding network around the polymer chain due to their large hydration diameters. However, K^+ and Cs^+ will have more disruptive effects on hydrogen bonding due to weaker hydration. Because our model does not explicitly account for the loss in the translational entropy of displaced solvent molecules, we expect that other effects are also approximated within $u_{i,i+1}$.

Besides the non-electrostatic energy, we assume that the effective screening parameter is dependent on the salt type (but not on the salt concentration). This parameter is related to the ability of the counterions to screen charge-charge interaction between monomers. We find that the screening parameter increases in value (i.e., stronger electrostatic screening) in the order of

$Li^+<Na^+<K^+<Cs^+$. Since the counterions have their own unique hydration structure, we expect that the ion size and local concentration must be responsible for the different effects of ion screening. The stronger hydration of counterions leads to a larger hard-sphere diameter thus an effective repulsion. In addition, the weakened screening of intrachain repulsion by Li^+ ions may be attributed to its strong binding with water molecules reducing the screening effects on charge-charge interactions. From best fitting of experimental titration data, we find the screening parameter τ_{cat^+} to be 0.257, 0.273, 0.462, and 0.857 for Li^+, Na^+, K^+, and Cs^+, respectively. Thus, the intrachain screening by the salt counterions is always weaker than the electrostatic screening predicted by the DH potential (viz. $\tau_{cat^+}=1$).

3.1 ***Titration of poly(acrylic acid) in different alkali chloride solutions***

Experiments have demonstrated that the choice of alkali metal influences the charging behavior of poly(acrylic acid). The ion-specific effect is particularly important at low salt concentrations where long-range intrachain interactions play a key role in the ionization of the polymer[30]. Since previous methods have relied on the DH potential to describe long-range interactions[22], they are unable to differentiate between different salt ions. In this work, we introduce a non-electrostatic energy $u_{i,i+1}$ to describe nearest-neighbor interactions and modify the long-range electrostatic interaction [Eq.(9)] by including an effective screening parameter τ_{cat^+} to account for the effect of different alkali cations on the charging behavior.

Figure 2 shows the titration curves of PAA (MW=88 kg/mol; *M*~1200) in four types of alkali chloride aqueous solutions (lithium, sodium, potassium, and cesium) at different salt concentrations[30]. With two adjustable parameters for each salt, the hierarchical model is able to reproduce the experimental titration curves at all salt concentrations. As expected, the degree of ionization increases at high pH or salt concentration. The salt concentration effect can be attributed

to the screening of Coulomb interactions between monomer segments along the polymer chain. The specific ion effects on the charging behavior of the polymer are most significant at low salt concentrations, suggesting that the long-range intrachain correlations lead to the difference in polymer charge with different salt ions. Our model can well capture the titration behavior of poly(acrylic acid) across all solution conditions owing to the successful description of both long-range interactions and the polymer conformation in a self-consistent manner.

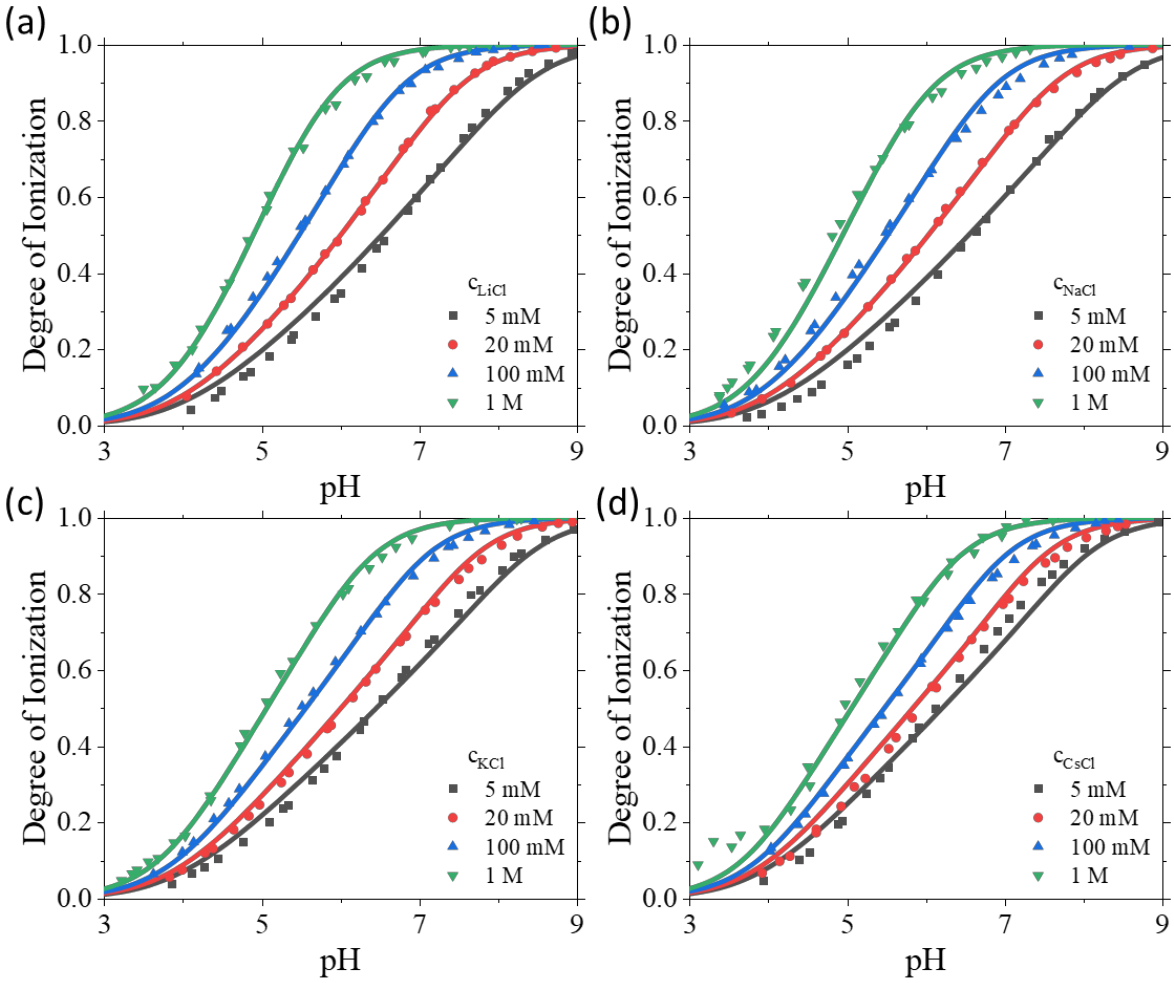

Figure 2. Titration curves for poly(acrylic acid) at 25 °C in the aqueous solutions of (a) lithium chloride, (b) sodium chloride, (c) potassium chloride, and (d) cesium chloride solutions from experiment (MW=88kg/mol)[30] (symbols) and theoretical correlations (*M*~1200) (lines).

Figure 3a shows the difference in the degree of ionization between PAA in 5 mM and 20 mM alkali chloride solutions. The theoretical results are compared with the prediction from the nearest-neighbor site-binding model (nnSB). Clearly, the ionization behavior of PAA differs significantly in the presence of different alkali metals. The significant salt concentration effect on ionization of PAA in LiCl compared to the other alkali metals originates from the weakened screening of Li^+ ions on the long-range intrachain interactions as described by parameter τ_{cat^+}. Conversely, the nearest-neighbor model is not able to capture specific salt effects without changing the polymer parameters; it predicts a much smaller change in the degree of ionization when the salt concentration is increased from 5 mM to 20 mM.

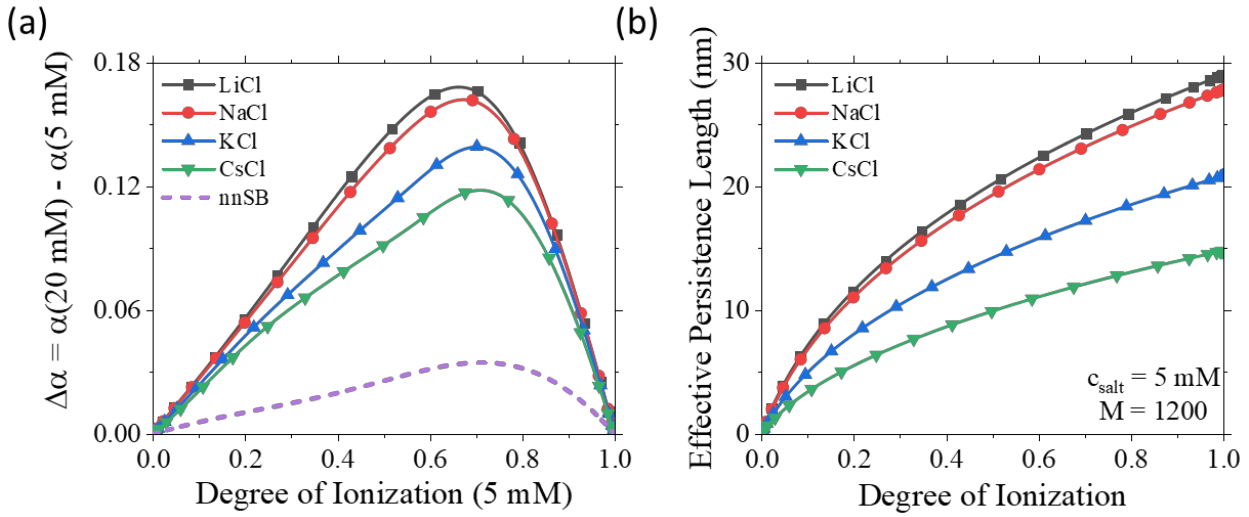

Figure 3. (a) The difference in degree of ionization of poly(acrylic acid) at 20 mM and 5 mM lithium chloride solution in four different salt solutions (viz. LiCl, NaCl, KCl, and CsCl). The dashed line is the prediction of the nearest-neighbor site-binding model (nnSB) for LiCl. (b) The effective persistence length of poly(acrylic acid) in a 5 mM salt solution.

Different from conventional site-binding models, our hierarchical model captures ionization effects on the conformation of the polymer at different alkali chloride solutions. Figure

3b presents the effective persistent length of PAA versus pH at a fixed salt concentration of 5 mM. Because the effective persistence length is directly related to the polymer size [υ in Eq.(18)], Figure 3b shows the polymer expansion is greatest in LiCl, decreasing from LiCl to CsCl because of different intrachain repulsion among ionizable segments. Our findings agree with a previous experimental study indicating that, at the same salt concentration, the radius of gyration of PAA decreases from LiCl to CsCl[44].

3.2 *Titration of poly(acrylic acid) in lithium chloride solution*

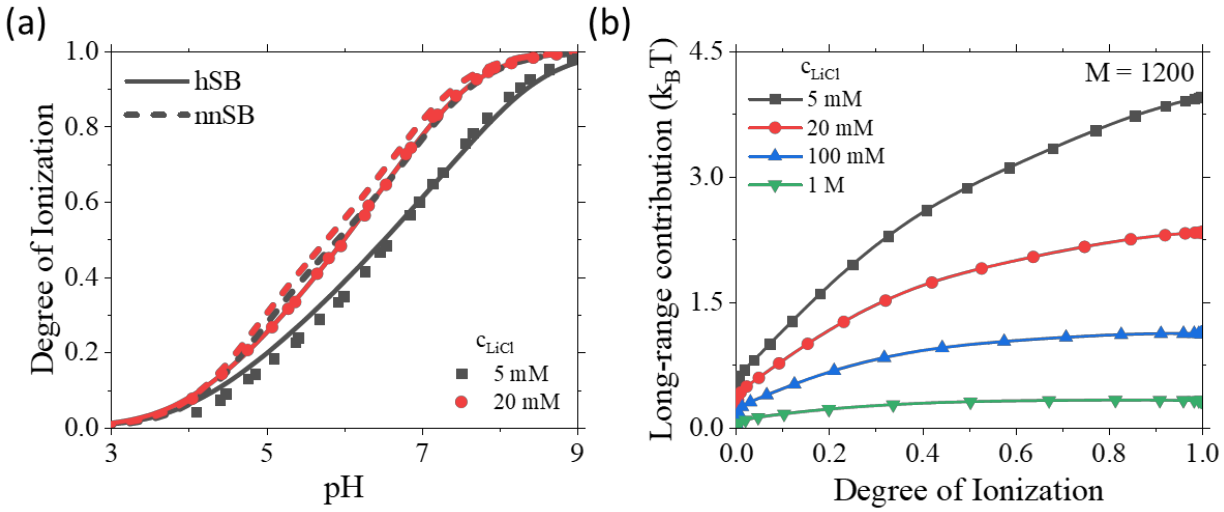

Figure 4. (a) The degree of ionization for poly(acrylic acid) in 5 mM and 20 mM lithium chloride solutions. The solid and dashed lines are the theoretical results for the hierarchical site-binding model (hSB) and the nearest-neighbor site-binding model (nnSB)[9], respectively. The symbols are experimental data for PAA (MW=88 kg/mol; M~1200). (b) The long-range contribution, x_i, i.e., non-neighboring contribution, to the free energy per segment versus the degree of ionization at four different lithium chloride concentrations.

To better understand the contribution due to long-range interactions, we compare the theoretical predictions for the hierarchical site-binding model (hSB) and nearest-neighbor site-binding model (nnSB) for the titration of poly(acrylic acid) (MW=88 kg/mol; *M*~1200). Figure 4a

shows the titration curves at two lithium chloride aqueous concentrations (5 mM and 20 mM), and Figure 4(b) shows the free energy per segment due to long-range interactions. While the nearest-neighbor model becomes unreliable at low salt concentration, the hierarchical model performs well at all salt concentrations indicating that the long-range interactions are properly accounted for. In general, the long-range contribution to the free energy of the system increases steadily with the degree of ionization due to the increased charge-charge interactions. Such effect diminishes as the salt concentration increases. At the lowest concentration considered in this work (viz. 5 mM), the long-range free energy increases up to around 2.5 k_BT per segment, which is equivalent to reducing the pH by 1 unit at full ionization. At 1 M LiCl, the contribution due to long-range interactions is negligible. In this case, the difference between the nearest-neighbor and our hierarchical site-binding model becomes insignificant because the charge-charge interaction is effectively screened. If the nearest-neighbor energy $W_{i,i+1}$ is grouped with non-neighboring interactions in $\Delta\Gamma$ (i.e., our model is developed by applying the perturbation to the non-interacting site-binding model thus $h_{i,j} = \alpha_i \alpha_j$), we find that the predicted results are quite similar to that shown in Figure 4a for our hierarchical site-binding model. Since poly(acrylic acid) has a low line charge density, the ionizable sites are not strongly correlated and an approximate treatment of site-site interactions is still satisfactory. We expect that this approximation would not hold for strongly correlated polymers such as poly(maleic acid) that exhibit a step-like titration curve.

The hierarchical site-binding model describes the ionization of a weak polyelectrolyte self-consistently with the change in polymer conformation. As shown in Figure 5(a), the polymer size, which is directly related to the effective persistence length, expands as the degree of ionization increases. Because the polymer expansion is primarily due to the electrostatic repulsion among the ionized monomers in the same polymer chain, it can be expected that the salt concentration plays

an important role in determining the size of the polymer chain. Figure 5(b) shows that the polymer behaves like an ideal gaussian chain with $\langle r_{i,j}^2 \rangle = (j-i)\sigma^2$ at low ionization and high salt concentration. On the other hand, the reduction in the salt concentration and increase in the degree of ionization would lead to a stronger intrachain repulsion and the polymer behaviors more like a rod-like chain with $\langle r_{i,j}^2 \rangle = (j-i)^2\sigma^2$. Our hierarchical site-binding model interpolates between these two limits by accounting for the entropic and electrostatic contributions to the polymer chain expansion.

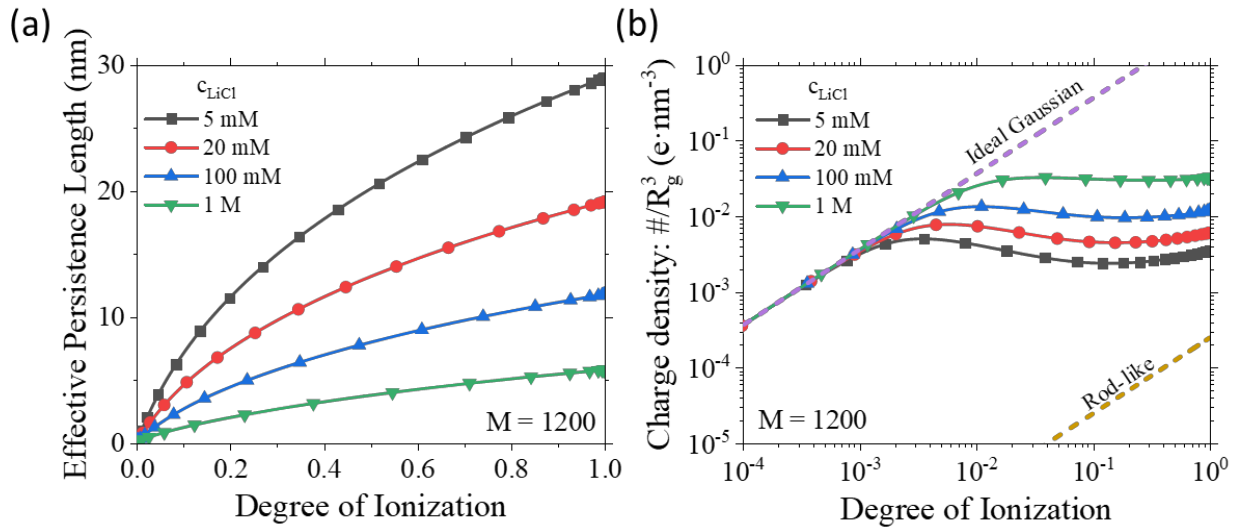

Figure 5. (a) The effective persistence length ℓ^{eff} and (b) the charge density for poly(acrylic acid) as determined through the hierarchical site-binding model as a function of degree of ionization at four different lithium chloride concentrations. Charge density is defined as $M\alpha_p e / \hat{R}_g^3$.

3.3 *Effect of chain length on ionization and conformation of PAA*

Lastly, we consider the polymer chain length effects on the ionization and conformation of poly(acrylic acid). According to the original site-binding model (nnSB), the chain has no significant effect on ionization when the weak polyelectrolyte contains more than 20 segments[21]. However, experimental results indicate a substantial chain length dependence on the titration of

most weak polyelectrolytes[18]. The failure of the nearest-neighbor model to capture the chain length effects can be attributed to its neglection of the long-range intrachain interactions. To illustrate, we show in Figure 6a the ionization behavior of PAA in a 0.1 mM lithium chloride solution at three different chain lengths (viz. M = 25, 75, and 1200). Our model predicts that increasing the chain length does lead to a noticeable reduction of the ionization at these solution conditions. The chain length effect is most significant at high degrees of ionization. Even at low degrees of ionization, there is a noticeable increase in resistance to ionization as the chain length increases. The reason for this is that, at the same degree of ionization, a longer chain will have a stronger intrachain repulsion due to the presence of more charged monomers ($n_{charged} = \alpha M$). Because the nearest-neighbor model does not account for long-range interactions, the chain length effect becomes irrelevant for PAA with $M > 20$.

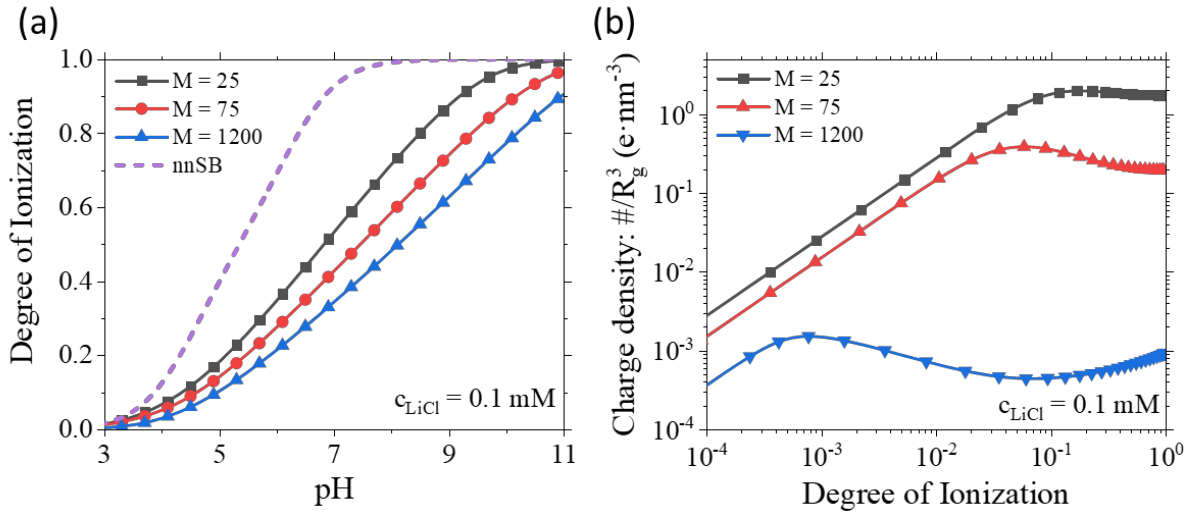

Figure 6. (a) The degree of ionization as a function of pH for three different chain lengths (M=25, 75, and 1200) in a 0.1 mM lithium chloride solution. The dashed line is predicted by the nearest-neighbor site-binding model (nnSB) which is independent of chain length at $M \geq 20$. (b) The charge density of the polymer as a function of degree of ionization for three different polymer chain lengths.

It has been previously demonstrated that the salt concentration has a substantial influence on the role that chain length may play on the ionization of weak polyelectrolytes[18]. The relevancy of salt concentration for the chain length effect is because the salt concentration limits the distance underpinning the long-range interactions. When the salt concentration is sufficiently high, a monomer interacts only with its immediate neighbors. On the other hand, if the salt concentration is low, the ionization is influenced by long-range interactions. Figure S1 shows the ionization behavior of PAA with different chain lengths at 100 mM. As discussed above, the chain length effect becomes less relevant as the salt concentration increases.

Owing to strong coupling between polymer ionization and conformation, the charge density of a weak polyelectrolyte is also highly dependent on the polymer chain length. For example, Figure 6b shows the charge density of PAA as a function of degree of ionization at three different chain lengths. Interestingly, the charge density exhibits a non-monotonic dependence on the degree of ionization when the chain length is sufficiently large. It decreases with the chain length because the total charge linearly scales with M at the same degree of ionization while the radius of gyration scales with $M^{0.5}$ when the polymer is mostly neutral. Thus, the charge density approximately scales with $M^{-0.5}$ at low degree of ionization. Similar to Figure 3b, the charge density increases almost linearly with degree of ionization when it follows the same behavior as an ideal gaussian chain. However, beyond certain charge density, the polymer expands more strongly due to intrachain repulsion and approaches another linear region when the polymer volume ($\sim R_g^3$) changes proportionally to the degree of ionization (i.e., charge density curve does not change with further ionization). The position at which the maximum in charge density occurs depends on the degree of ionization, but corresponds to when the polymer has approximately 4-5

monomers charged regardless of the chain length. While the long chain polymer ($M = 1200$) shows a noticeable maximum in charge density with degree of ionization, the maximum is relatively insignificant for the short chain ($M = 25$) due to the small entropic penalty that occurs for the expansion of the polymer as the chain length increases. Clearly a sufficient driving force (viz. repulsive charge-charge interactions) is necessary to overcome the entropic penalty for expansion of the polymer.

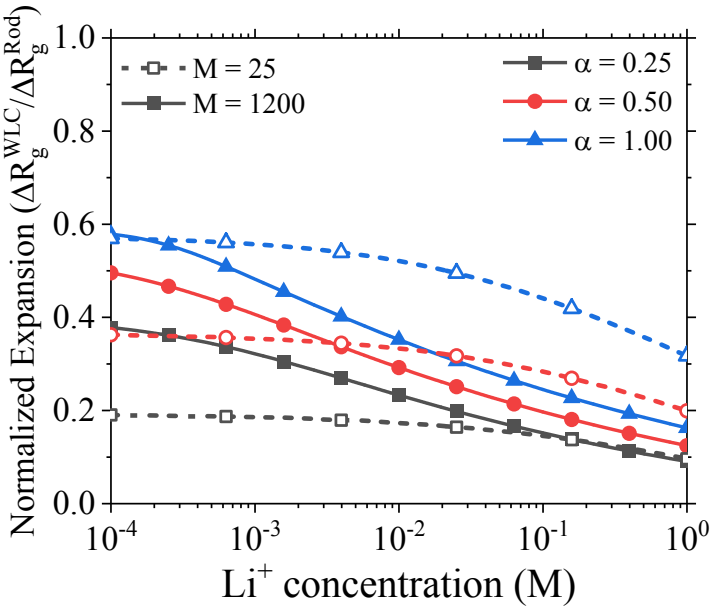

Figure 7. The normalized expansion defined as the ratio of the difference in radius of gyration between the worm-like chain (WLC) and the ideal Gaussian chain ($R_g^{WLC} - R_g^{ideal}$) over the difference of the rod-like chain and the ideal Gaussian chain ($R_g^{Rod} - R_g^{ideal}$) at different concentrations of lithium ions for three different degrees of ionization and two different chain lengths.

To better understand the difference in the conformation of the short chain ($M = 25$) and long chain ($M = 1200$) weak polyelectrolytes, we show in Figure 7 the normalized expansion

$\Delta R_g^{WLC} / \Delta R_g^{Rod}$, where $\Delta R_g^{***} = R_g^{***} - R_g^{ideal}$, versus the Li^+ concentration at different stages of ionization. When the normalized expansion is close to zero, the polymer conformation is similar to that of an ideal chain, whereas a value close to unity means that the polymer adopts a rod-like conformation, i.e., it is significantly stretched. As expected, an increase in ionization leads to a higher value for the normalized expansion (i.e., towards to the rod-like limit) due to the stronger intramolecular repulsion. On the other hand, the increase in salt concentration reduces the normalized expansion (i.e., towards the ideal-chain limit). It should be noted that as the salt concentration falls, we must increase the solution pH in order to maintain the same degree of ionization. As a result, more counterions (i.e., lithium ions) must be added in order to satisfy the charge neutrality due to the added hydroxyl ions. At high pH, the proton concentration is much smaller than that of hydroxyl ions ($c_{OH^-} >> c_{H^+}$), the actual concentration of lithium ions is much higher than the chloride concentration. At dilute salt concentrations, the normalized expansion approaches a limit different from that corresponding to the rod conformation due to the tradeoff between intrachain repulsion and the entropic penalty in adopting a single polymer conformation. Increasing the chain length generally results in further expansion (i.e., deviation from the gaussian limit) at dilute salt concentrations since there is more charged monomers to interact with. However, there is a limit since the repulsion between the monomers at large separation may not be enough to compete with the entropic penalty for further expansion. As expected, a higher degree of ionization (i.e., a closer spacing between charged sites in the polymer backbone) leads to a polymer conformation closer to the rod limit.

Figure 7 indicates that the behavior of weak polyelectrolyte expansion is highly sensitive to the salt concentration. At dilute salt conditions, a long chain is more responsive to the polymer charge than a short chain. However, at high salt conditions, a long polymer chain does not expand

as significantly as the short chain. The reason for the weaker expansion at high salt concentration can be attributed to the range and strength of the long-range interactions as well as the greater conformational freedom when the chain length is increased. When the salt concentration is low, the long-range intrachain interactions promote the polymer expansion and the polymer expands relative to resistance due to entropic forces. At high salt concentration, the long-range interactions quickly decay due to the shortened screening length (κ^{-1}) and therefore these long-range interactions are not as relevant. As shown in Figure 6b, at the same degree of ionization, the charge density of the polymer decreases with an increase in chain length. Therefore, the smaller expansion of the long chain polymer at high salt concentration can be attributed to the fact that the charged sites are further apart from one another than in the short-chain case. In fact, the greater separation between charged sites is also the reason that the normalized expansion begins to decrease at an earlier salt concentration for the long chain than the short chain. A similar explanation can be applied to why the salt concentration shows less influence on the short chain expansion since the charged sites are closer to one another and therefore the interactions cannot be sufficiently screened. Thus, a theoretical model that accounts for intrachain repulsion and polymer conformation is vital to the correct description of weak polyelectrolytes.

4. Conclusions

We have developed a generalized site-binding model to account for the ionization and conformational behavior of weak polyelectrolytes through a self-consistent description of the inter- and intramolecular correlations, ionization energy and polymer conformation. The hierarchical model improves upon conventional site-binding methods by incorporating the polymer conformation and long-range intrachain correlations (i.e., between non-neighboring segments). It achieves the ionization and conformation consistency by adopting a worm-like chain model with

the non-nearest neighbor interactions evaluated through the Gibbs-Bogoliubov variational principle. Importantly, the hierarchical model captures the influence of solution conditions on the inter- and intramolecular correlations of the polymer through the augmented primitive model of aqueous solutions. With two parameters describing salt-specific nearest-neighbor interactions and non-electrostatic screening effects, the hierarchical model provides quantitative predictions both ionization and polymer expansion for weak polyelectrolytes in different salt solutions as well as at different salt concentrations. With the ionization potential and nearest-neighbor energy changing with solution conditions, the conventional site-binding model works well at moderate to high salt conditions. However, the conventional model ignores polymer conformation and long-range intrachain correlations that are deemed inadequate at low salt concentration. Our hierarchical model maintains good performance at low salt concentrations since it accounts for polymer expansion and the long-range correlations explicitly.

In this work, we have focused our attention towards poly(acrylic acid), a linear polyacid with a relatively low density of ionizable sites along the backbone (i.e., weakly correlated). Poly(acrylic acid) serves as a reasonable starting point to investigate other weak polyelectrolyte systems including strongly correlated polymers like poly(maleic acid) that exhibit stereochemical-dependent features as well as hetero-weak polyelectrolytes such as zwitterionic polymers. The long-range correlations are particularly important for the latter since conventional methods that truncate at the nearest-neighbor level will miss the attractive and repulsive interactions between non-adjacent sites. Recently, Lunkad et al. demonstrated the importance of considering long-range interactions by showing the similarity in titration behavior of a block copolymer with one block containing acidic monomers and the other block containing basic monomers versus a polymer with alternating acidic and basic monomers[51]. Molecular architectures besides the linear polymer such

as star-like polymers or dendrimers are also of importance due to their practical interest[7, 14]. While this model is a significant advancement over conventional methods, the explicit coupling of long-range interactions and spatial configuration of the polymer is only implicitly accounted for through the effective persistence length parameter. We are currently pursuing further development along these directions.

Conflicts of interest:

There are no conflicts to declare.

Acknowledgements:

This work is financially supported by the NSF-DFG Lead Agency Activity in Chemistry and Transport in Confined Spaces under Grant No. NSF 2234013. Additional support is provided by the NSF Graduate Research Fellowship under Grant No. DGE-1326120.

Supporting Information:

Full set of equations for determining the excess chemical potential due to electrostatic correlations, two-body correlation terms, the local electric potential, the grand potential and correlation functions of the near-neighbor model, and the Gibbs-Bogoliubov variational principle.

References:

1. Kord Forooshani, P.; Lee, B. P., Recent Approaches in Designing Bioadhesive Materials Inspired by Mussel Adhesive Protein. *Journal of polymer science. Part A, Polymer chemistry* **2017**, *55*, 9-33.
2. Priya James, H.; John, R.; Alex, A.; Anoop, K. R., Smart Polymers for the Controlled Delivery of Drugs – a Concise Overview. *Acta Pharmaceutica Sinica B* **2014**, *4*, 120-127.
3. Bolto, B.; Gregory, J., Organic Polyelectrolytes in Water Treatment. *Water Research* **2007**, *41*, 2301-2324.
4. Seitz, S.; Ajiro, H., Self-Assembling Weak Polyelectrolytes for the Layer-by-Layer Encapsulation of Paraffin-Type Phase Change Material Icosane. *Solar Energy Materials and Solar Cells* **2019**, *190*, 57-64.
5. Jaganathan, S., Bioresorbable Polyelectrolytes for Smuggling Drugs into Cells. *Artificial Cells, Nanomedicine, and Biotechnology* **2016**, *44*, 1080-1097.

6. de Groot, J.; Koper, G. J. M.; Borkovec, M.; de Bleijser, J., Dissociation Behavior of Poly(Maleic Acid): Potentiometric Titrations, Viscometry, Pulsed Field Gradient Nmr, and Model Calculations. *Macromolecules* **1998**, *31*, 4182-4188.
7. van Duijvenbode, R. C.; Borkovec, M.; Koper, G. J. M., Acid-Base Properties of Poly(Propylene Imine)Dendrimers. *Polymer* **1998**, *39*, 2657-2664.
8. Borkovec, M.; Koper, G. J. M.; Piguet, C., Ion Binding to Polyelectrolytes. *Current Opinion in Colloid & Interface Science* **2006**, *11*, 280-289.
9. Gallegos, A.; Ong, G. M. C.; Wu, J., Thermodynamic Non-Ideality in Charge Regulation of Weak Polyelectrolytes. *Soft Matter* **2021**, *17*, 9221-9234.
10. Gonzalez Solveyra, E.; Nap, R. J.; Huang, K.; Szleifer, I., Theoretical Modeling of Chemical Equilibrium in Weak Polyelectrolyte Layers on Curved Nanosystems. *Polymers* **2020**, *12*, 2282.
11. Landsgesell, J.; Nová, L.; Rud, O.; Uhlík, F.; Sean, D.; Hebbeker, P.; Holm, C.; Košovan, P., Simulations of Ionization Equilibria in Weak Polyelectrolyte Solutions and Gels. *Soft Matter* **2019**, *15*, 1155-1185.
12. Nap, R. J.; Park, S. H.; Szleifer, I., Competitive Calcium Ion Binding to End-Tethered Weak Polyelectrolytes. *Soft Matter* **2018**, *14*, 2365-2378.
13. Rathee, V. S.; Zervoudakis, A. J.; Sidky, H.; Sikora, B. J.; Whitmer, J. K., Weak Polyelectrolyte Complexation Driven by Associative Charging. *The Journal of Chemical Physics* **2018**, *148*, 114901.
14. Uhlík, F.; Košovan, P.; Limpouchová, Z.; Procházka, K.; Borisov, O. V.; Leermakers, F. A. M., Modeling of Ionization and Conformations of Starlike Weak Polyelectrolytes. *Macromolecules* **2014**, *47*, 4004-4016.
15. Gallegos, A.; Ong, G. M. C.; Wu, J., Ising Density Functional Theory for Weak Polyelectrolytes with Strong Coupling of Ionization and Intrachain Correlations. *The Journal of Chemical Physics* **2021**, *155*, 241102.
16. Hyltegren, K.; Skepö, M., Adsorption of Polyelectrolyte-Like Proteins to Silica Surfaces and the Impact of Ph on the Response to Ionic Strength. A Monte Carlo Simulation and Ellipsometry Study. *Journal of Colloid and Interface Science* **2017**, *494*, 266-273.
17. Carnal, F.; Stoll, S., Adsorption of Weak Polyelectrolytes on Charged Nanoparticles. Impact of Salt Valency, Ph, and Nanoparticle Charge Density. Monte Carlo Simulations. *The Journal of Physical Chemistry B* **2011**, *115*, 12007-12018.
18. Laguecir, A.; Ulrich, S.; Labille, J.; Fatin-Rouge, N.; Stoll, S.; Buffle, J., Size and Ph Effect on Electrical and Conformational Behavior of Poly(Acrylic Acid): Simulation and Experiment. *European Polymer Journal* **2006**, *42*, 1135-1144.
19. Brush, S. G., History of the Lenz-Ising Model. *Reviews of modern physics* **1967**, *39*, 883.
20. Cipra, B. A., An Introduction to the Ising Model. *The American Mathematical Monthly* **1987**, *94*, 937-959.
21. Koper, G. J. M.; Borkovec, M., Proton Binding by Linear, Branched, and Hyperbranched Polyelectrolytes. *Polymer* **2010**, *51*, 5649-5662.
22. Garcés, J. L.; Madurga, S.; Rey-Castro, C.; Mas, F., Dealing with Long-Range Interactions in the Determination of Polyelectrolyte Ionization Properties. Extension of the Transfer Matrix Formalism to the Full Range of Ionic Strengths. *Journal of Polymer Science Part B: Polymer Physics* **2017**, *55*, 275-284.
23. Gallegos, A.; Wu, J., Molecular Thermodynamics for Amino-Acid Adsorption at Inorganic Surfaces. *AIChE Journal* **2021**, e17432.

24. Gallegos, A.; Wu, J., Charge Regulation of Natural Amino Acids in Aqueous Solutions. *Journal of Chemical & Engineering Data* **2020**.
25. Simonin, J.-P.; Blum, L.; Turq, P., Real Ionic Solutions in the Mean Spherical Approximation. 1. Simple Salts in the Primitive Model. *The Journal of Physical Chemistry* **1996**, *100*, 7704-7709.
26. Lide, D. R., *Crc Handbook of Chemistry and Physics*; CRC press, 2004; Vol. 85.
27. Blum, L., Mean Spherical Model for Asymmetric Electrolytes. *Molecular Physics* **1975**, *30*, 1529-1535.
28. Maribo-Mogensen, B.; Kontogeorgis, G. M.; Thomsen, K., Comparison of the Debye–Hückel and the Mean Spherical Approximation Theories for Electrolyte Solutions. *Industrial & Engineering Chemistry Research* **2012**, *51*, 5353-5363.
29. Kawaguchi, S.; Kitano, T.; Ito, K.; Minakata, A., Dissociation Behavior of Poly (Fumaric Acid) and Poly (Maleic Acid). Ii. Model Calculation. *Macromolecules* **1990**, *23*, 731-738.
30. Sadeghpour, A.; Vaccaro, A.; Rentsch, S.; Borkovec, M., Influence of Alkali Metal Counterions on the Charging Behavior of Poly(Acrylic Acid). *Polymer* **2009**, *50*, 3950-3954.
31. Yu, Y.-X.; Wu, J.; Gao, G.-H., Density-Functional Theory of Spherical Electric Double Layers and Z Potentials of Colloidal Particles in Restricted-Primitive-Model Electrolyte Solutions. *The Journal of chemical physics* **2004**, *120*, 7223-7233.
32. Henderson, D.; Smith, W. R., Exact Analytical Formulas for the Distribution Functions of Charged Hard Spheres in the Mean Spherical Approximation. *Journal of Statistical Physics* **1978**, *19*, 191-200.
33. Blanco, P. M.; Madurga, S.; Mas, F.; Garcés, J. L., Coupling of Charge Regulation and Conformational Equilibria in Linear Weak Polyelectrolytes: Treatment of Long-Range Interactions Via Effective Short-Ranged and Ph-Dependent Interaction Parameters. *Polymers* **2018**, *10*, 811.
34. Blanco, P. M.; Madurga, S.; Mas, F.; Garcés, J. L., Effect of Charge Regulation and Conformational Equilibria in the Stretching Properties of Weak Polyelectrolytes. *Macromolecules* **2019**, *52*, 8017-8031.
35. Blanco, P. M.; Madurga, S.; Narambuena, C. F.; Mas, F.; Garcés, J. L., Role of Charge Regulation and Fluctuations in the Conformational and Mechanical Properties of Weak Flexible Polyelectrolytes. *Polymers* **2019**, *11*, 1962.
36. Chandler, D., Introduction to Modern Statistical. *Mechanics. Oxford University Press, Oxford, UK* **1987**, *5*.
37. Yamakawa, H., *Modern Theory of Polymer Solutions*; Harper & Row, 1971.
38. Wang, Z.-G., 50th Anniversary Perspective: Polymer Conformation—a Pedagogical Review. *Macromolecules* **2017**, *50*, 9073-9114.
39. Shen, K.; Wang, Z.-G., Polyelectrolyte Chain Structure and Solution Phase Behavior. *Macromolecules* **2018**, *51*, 1706-1717.
40. Shen, K.; Wang, Z.-G., Electrostatic Correlations and the Polyelectrolyte Self Energy. *The Journal of chemical physics* **2017**, *146*, 084901.
41. Flory, P. J., *Principles of Polymer Chemistry*; Cornell University Press, 1953.
42. De Gennes, P. d., Collapse of a Polymer Chain in Poor Solvents. *Journal de Physique Lettres* **1975**, *36*, 55-57.
43. Blaakmeer, J.; Bohmer, M. R.; Stuart, M. C.; Fleer, G., Adsorption of Weak Polyelectrolytes on Highly Charged Surfaces. Poly (Acrylic Acid) on Polystyrene Latex with Strong Cationic Groups. *Macromolecules* **1990**, *23*, 2301-2309.

44. Kim, H. G.; Lee, J. H.; Lee, H. B.; Jhon, M. S., Dissociation Behavior of Surface-Grafted Poly(Acrylic Acid): Effects of Surface Density and Counterion Size. *Journal of Colloid and Interface Science* **1993**, *157*, 82-87.
45. Wu, T.; Gong, P.; Szleifer, I.; Vlcˇek, P.; Šubr, V.; Genzer, J., Behavior of Surface-Anchored Poly (Acrylic Acid) Brushes with Grafting Density Gradients on Solid Substrates: 1. Experiment. *Macromolecules* **2007**, *40*, 8756-8764.
46. Léonforte, F.; Welling, U.; Müller, M., Single-Chain-in-Mean-Field Simulations of Weak Polyelectrolyte Brushes. *The Journal of Chemical Physics* **2016**, *145*, 224902.
47. Gong, P.; Wu, T.; Genzer, J.; Szleifer, I., Behavior of Surface-Anchored Poly (Acrylic Acid) Brushes with Grafting Density Gradients on Solid Substrates: 2. Theory. *Macromolecules* **2007**, *40*, 8765-8773.
48. Lützenkirchen, J.; van Male, J.; Leermakers, F.; Sjöberg, S., Comparison of Various Models to Describe the Charge−Ph Dependence of Poly(Acrylic Acid). *Journal of Chemical & Engineering Data* **2011**, *56*, 1602-1612.
49. Kitano, T.; Kawaguchi, S.; Ito, K.; Minakata, A., Dissociation Behavior of Poly(Fumaric Acid) and Poly(Maleic Acid). 1. Potentiometric Titration and Intrinsic Viscosity. *Macromolecules* **1987**, *20*, 1598-1606.
50. Marcus, Y., Thermodynamics of Solvation of Ions. Part 5.—Gibbs Free Energy of Hydration at 298.15 K. *Journal of the Chemical Society, Faraday Transactions* **1991**, *87*, 2995-2999.
51. Lunkad, R.; Murmiliuk, A.; Tošner, Z.; Štěpánek, M.; Košovan, P., Role of Pka in Charge Regulation and Conformation of Various Peptide Sequences. *Polymers* **2021**, *13*, 214.